Analysis of core circadian feedback loop in suprachiasmatic nucleus of mCry1-luc transgenic reporter mouse

Elizabeth S. Maywood, Lesley Drynan, Johanna E. Chesham, Mathew D. Edwards, Hugues Dardente, Jean-Michel Fustin, David G. Hazlerigg, John S. O'Neill, Gemma F. Codner, Nicola J. Smyllie, et al.

Analysis of core circadian feedback loop in suprachiasmatic nucleus of *mCry1-luc* transgenic reporter mouse

Elizabeth S. Maywood[a], Lesley Drynan[a], Johanna E. Chesham[a], Mathew D. Edwards[a], Hugues Dardente[b], Jean-Michel Fustin[b], David G. Hazlerigg[b], John S. O'Neill[c], Gemma F. Codner[d], Nicola J. Smyllie[a], Marco Brancaccio[a], and Michael H. Hastings[a,1]

[a]Neurobiology Division, Medical Research Council Laboratory of Molecular Biology, Cambridge CB2 0QH, United Kingdom; [b]Institute of Biological and Environmental Sciences, University of Aberdeen, Aberdeen AB24 2TZ, United Kingdom; [c]Cell Biology Division, Medical Research Council Laboratory of Molecular Biology, Cambridge CB2 0QH, United Kingdom; and [d]Mary Lyon Centre, Medical Research Council Harwell, Oxfordshire OX11 0RD, United Kingdom

Edited by Joseph S. Takahashi, Howard Hughes Medical Institute, University of Texas Southwestern Medical Center, Dallas, TX, and approved May 1, 2013 (received for review December 4, 2012)

The suprachiasmatic nucleus (SCN) coordinates circadian rhythms that adapt the individual to solar time. SCN pacemaking revolves around feedback loops in which expression of *Period* (*Per*) and *Cryptochrome* (*Cry*) genes is periodically suppressed by their protein products. Specifically, PER/CRY complexes act at E-box sequences in *Per* and *Cry* to inhibit their transactivation by CLOCK/BMAL1 heterodimers. To function effectively, these closed intracellular loops need to be synchronized between SCN cells and to the light/dark cycle. For *Per* expression, this is mediated by neuropeptidergic and glutamatergic extracellular cues acting via cAMP/calcium-responsive elements (CREs) in *Per* genes. *Cry* genes, however, carry no CREs, and how CRY-dependent SCN pacemaking is synchronized remains unclear. Furthermore, whereas reporter lines are available to explore *Per* circadian expression in real time, no *Cry* equivalent exists. We therefore created a mouse, B6.Cg-Tg(Cry1-luc)01Ld, carrying a transgene (*mCry1-luc*) consisting of *mCry1* elements containing an E-box and E′-box driving firefly luciferase. *mCry1-luc* organotypic SCN slices exhibited stable circadian bioluminescence rhythms with appropriate phase, period, profile, and spatial organization. In SCN lacking vasoactive intestinal peptide or its receptor, *mCry1* expression was damped and desynchronized between cells. Despite the absence of CREs, *mCry1-luc* expression was nevertheless (indirectly) sensitive to manipulation of cAMP-dependent signaling. In *mPer1/2*-null SCN, *mCry1-luc* bioluminescence was arrhythmic and no longer suppressed by elevation of cAMP. Finally, an SCN graft procedure showed that PER-independent as well as PER-dependent mechanisms could sustain circadian expression of *mCry1*. The *mCry1-luc* mouse therefore reports circadian *mCry1* expression and its interactions with vasoactive intestinal peptide, cAMP, and PER at the heart of the SCN pacemaker.

gene expression | period gene | adenylate cyclase | VPAC2 | afterhours

The suprachiasmatic nucleus (SCN) of the hypothalamus is the principal circadian pacemaker in mammals, coordinating daily programs of gene expression across the body that ultimately underpin adaptation to day and night (1). SCN pacemaking revolves around an autoregulatory feedback loop in which expression of *Period* (*Per*) and *Cryptochrome* (*Cry*) genes is suppressed by their protein products on a daily basis. Specifically, PER/CRY complexes act at E-box regulatory sequences in *Per* and *Cry* to inhibit their transactivation by CLOCK/BMAL1 heterodimers (2). Supplementary feedback loops involving bZIP-family proteins [albumin D-element binding protein (*Dbp*) and nuclear factor, interleukin 3 regulated (*Nfil3*) acting at D-boxes] and REV-ERB family nuclear receptors (acting at RORE elements) confer additional robustness and amplitude (3), but E-box–mediated transcription is the principal determinant of SCN molecular pacemaking.

To generate a coherent circadian signal across the SCN, the intracellular loops are synchronized between cells by neuropeptidergic cues that act via signaling cascades triggered by cAMP and intracellular Ca^{2+} ($[Ca^{2+}]_i$) (4, 5). In addition, synchronization to the cycle of light and darkness is mediated by specialized glutamatergic retinal innervation of SCN neurons (6) that acts via $[Ca^{2+}]_i$ (7). These cAMP/$[Ca^{2+}]_i$ pathways converge upon cAMP/calcium-responsive elements (CREs) in the *Per* genes (8) to activate their expression (9). Thus, extracellular synchronizing stimuli gain access to the PER-dependent components of the feedback loops. *Cry* genes, however, carry no CREs as access points for extracellular information, raising the question of how CRY-dependent elements of the SCN pacemaker are synchronized. Consistent with a model of indirect regulation, reentrainment of daily *Cry* expression in the SCN of mice subjected to phase-advanced lighting cycles lags behind *Per* rhythms (10). *Cry* expression requires several days to resynchronize, but, importantly, the time course of *mCry* reentrainment parallels that of the rest–activity cycle, highlighting the contribution of *Cry* expression to the timing of behavior.

A comprehensive understanding of the SCN circadian pacemaker in toto requires, therefore, direct and dynamic analyses of *Cry* gene expression, but whereas various mouse lines (11, 12) have been powerful tools in examining *Per* expression, no reporter lines are available with which to characterize intra- and intercellular mechanisms governing *mCry1* expression. We therefore generated a transgenic (Tg) mouse line, B6.Cg-Tg(Cry1-luc)^{01Ld}, carrying a *mCry1-luciferase* bioluminescent reporter, using previously characterized *Cry1* elements that contain an E-box and E′-box (13) with an overlapping D-box (14). We show that these sequences are sufficient to drive period- and phase-appropriate circadian cycles of *mCry1* transcription consistent with E-box regulation in organotypic SCN and peripheral tissue cultures. Despite lacking CRE sequences, *mCry1* circadian transcription in the SCN was nevertheless dependent upon signaling via vasoactive intestinal peptide (VIP) and its VPAC2 receptor, a positive regulator of adenylyl cyclase (AC). Moreover, direct pharmacological manipulation of cAMP levels, both positive and negative, disrupted circadian *mCry1* expression. In the absence of mPER1 and mPER2 proteins, however, *mCry1-luc* transcription in the SCN was arrhythmic and no longer suppressed by elevated cAMP levels, highlighting a role for mPER1 and mPER2 as transducers in the circadian regulation of *mCry1*. Finally, by using an SCN slice grafting technique, we show that mPER1/mPER2-

Author contributions: E.S.M., M.D.E., J.S.O., M.B., and M.H.H. designed research; E.S.M., L.D., J.E.C., M.D.E., H.D., G.F.C., N.J.S., M.B., and M.H.H. performed research; H.D., J.-M.F., and D.G.H. contributed new reagents/analytic tools; E.S.M., L.D., J.E.C., M.D.E., N.J.S., M.B., and M.H.H. analyzed data; and E.S.M., L.D., H.D., J.S.O., and M.H.H. wrote the paper.

The authors declare no conflict of interest.

This article is a PNAS Direct Submission.

Freely available online through the PNAS open access option.

[1]To whom correspondence should be addressed. E-mail: mha@mrc-lmb.cam.ac.uk.

This article contains supporting information online at www.pnas.org/lookup/suppl/doi:10.1073/pnas.1220894110/-/DCSupplemental.

independent pathways could also sustain circadian expression of *mCry1*. Thus, parallel PER-dependent and PER-independent pathways direct circadian expression of mCRY1, the principal negative feedback regulator in the SCN.

Results

Period and Phase of SCN Circadian mCry1-luc Expression. Following injection of mouse oocyte (strain B6CBAF1/OlaHsd) with linearized plasmid carrying −1,504 to +107 of *mCry1* upstream of luciferase coding sequence (Fig. S1*A*), and subsequent embryo transfer, six transgenic founder mice were identified and crossed with nontransgenic mice to establish breeding lines. Of these, three lines produced offspring with a bioluminescent signal detectable in the SCN, and the line with the most intense SCN signal was selected for further analysis. All subsequent crosses (greater than six) were with mice on a C57BL/6 background to create the B6.Cg-Tg(Cry1-luc)^{01Ld} (*mCry1-luc*) line, which bred true, and digital droplet PCR identified a single copy of the reporter construct at a single insertion.

When recorded by photomultiplier array, all SCN slices carrying the reporter (n = 28) on an otherwise WT background exhibited stable bioluminescence rhythms (Fig. 1*A*) with periods within the circadian range (mean ± SEM, 24.21 ± 0.08 h) that were not significantly different from those of the widely used mPER2::LUC fusion protein reporter (12) (24.40 ± 0.04 h; $n = 11$; *t* test, $P = 0.16$), although they were more variable between slices than mPER2::LUC reports (range *mCry1-luc*, 22.89–24.99 h; mPER2::LUC, 24.13–24.59 h; SD, 0.42 vs. 0.12). *mCry1*-driven bioluminescence tended to be lower than that of mPER2::LUC SCN (2,940 ± 403 cps vs. 3,908 ± 521 cps; 75.2%) but not statistically so (*t* test, $P = 0.19$). The amplitude of the oscillation was, however, significantly smaller than that of mPER2::LUC (403 ± 49 cps vs. 2,377 ± 270 cps; *t* test, $P < 0.01$), and the relative amplitude error (RAE) was significantly higher in *mCry1-luc* slices (0.050 ± 0.004 vs. 0.033 ± 0.002; $P < 0.01$), indicative of lower cycle-to-cycle signal reproducibility. The relative decline of peak height (which arises from use of luciferin substrate) was calculated in a subset of recordings and followed the same exponential decay for both reporters (both $r^2 = 0.99$; Fig. 1*B*). A one-phase exponential decay half-life showed no significant difference between reporters (*mCry1-luc*, 2.27 ± 0.69 d; mPER2::LUC, 3.00 ± 0.42 d; *t* test, $P = 0.44$; $n = 9$ and $n = 6$, respectively).

Importantly, the *mCry1-luc* transgene faithfully reported the effects of two mutant alleles on SCN circadian period (Fig. 1*C* and Fig. S1*B*). The *Tau* allele of *casein kinase 1*ε (*CK1*ε^{Tau}) allele dose-dependently accelerated pacemaking by approximately 2.2 h per copy (15), whereas the *Afterhours* allele of *Fbxl3* (*Fbxl3*^{Afh}) slowed the SCN by approximately 2.1 h per copy (16). Deceleration by the *Fbxl3*^{Afh} mutation was also accompanied by a prolongation of the nadir of bioluminescence [WT, 6.40 ± 0.63 h; heterozygote, 8.13 ± 0.13 h; homozygote, 10.00 ± 0.32 h (mean ± SEM); $n = 4$, $n = 3$, and $n = 4$, respectively]. This reflects an extended phase of negative feedback on the E-boxes of the transgene caused by Afh-stabilized CRY proteins. Despite these differences in period, there was no difference in the quality of the rhythms reported by *mCry1-luc* (RAE, WT, 0.050 ± 0.004, $n = 28$; *Tau* homozygote, 0.054 ± 0.008, $n = 6$; *Afh* homozygote, 0.051 ± 0.007, $n = 5$).

In the SCN in vivo, expression of *mCry1* mRNA peaks later in the circadian day, at approximately circadian time 10 to 12, whereas *mPer1* mRNA levels peak earlier, at approximately circadian time 06 (17, 18). To determine the phase reported by the transgene in vitro, SCN from *mCry1-luc* and *mPer1-luc* mice were treated with forskolin and isobutyl-1-methylxanthine (IBMX) for 8 d and then transferred to fresh, drug-free medium. This treatment synchronizes previously unsynchronized SCN slices to a single-phase (19). This was evident within the separate groups of SCN carrying *mCry1* or *mPer1* reporters (Fig. S1*C*). Comparison between the groups, however, revealed a phase difference, such that the *mCry1*-reported rhythm was 5.3 ± 0.6 h delayed relative to the *mPer1-luc* cycle ($P < 0.01$, *t* test; $n = 3$ per reporter; Fig. 1*D*). Assuming that the time for translation and activation of luciferase is the same in the two reporters, the *mCry1-luc* peak is exactly in the phase predicted by the respective mRNA peaks (*mCry1* delayed relative to *mPer1* by 4–6 h). Therefore, as in cell culture (13), the *mCry1-luc* construct was sufficient to sustain the phase relationship observed in vivo. Thus, the circadian activation of the *mCry1-luc* transgene within the SCN slice of B6.Cg-Tg(Cry1-luc)^{01Ld} mice is of appropriate period, profile, and phase to that observed in vivo, providing a high-fidelity tool with which to analyze E-box–mediated circadian control of *mCry1* within the SCN. Finally, consistent with the earlier validation of the reporter in 3T3 cells (13), the majority of peripheral tissue explants from *mCry1-luc* mice exhibited circadian bioluminescence rhythms (Fig. S1*D*). As for SCN, the overall level of bioluminescence and circadian period were not different from corresponding mPER2::LUC explants, but amplitude and coherence were significantly lower (Tables S1 and S2). Finally, *mCry1-luc* MEFs exhibited clear circadian cycles of bioluminescence (Fig. S1*E* and Table S3) comparable to those of mPER2::LUC but with higher amplitude that progressively damped and were reactivated by medium change.

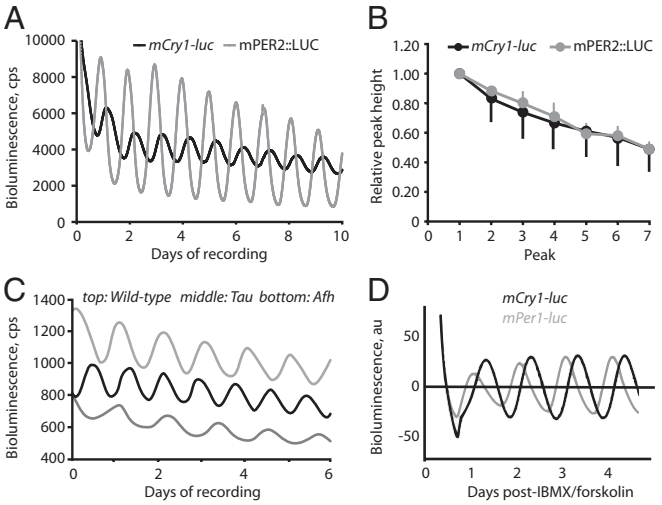

Fig. 1. Circadian period and phase of *mCry1-luc* expression in SCN. (*A*) Representative bioluminescence recordings from *mCry1-luc* and mPER2::LUC SCN slices. (*B*) Relative decline in signal amplitude caused by substrate use from *mCry1-luc* and mPER2::LUC SCN ($n = 10$ for both; data normalized to initial value of 100%; mean ± SD). (*C*) Representative bioluminescence recordings from WT (gray), *CK1*ε^{Tau} (black), and *Fbxl3*^{Afh} (dark gray) *mCry1-luc* SCN. (*D*) Representative recordings of baseline-corrected bioluminescence from *mCry1-luc* and *mPer1-luc* SCN following washout of forskolin/IBMX. Note later phase of *mCry1-luc*.

Spatiotemporal Control of SCN mCry1 Circadian Activation. Immunofluorescent staining for luciferase and CCD imaging revealed *mCry1-luc* activation across the SCN (Fig. 2 *A* and *B*), with expression in arginine vasopressin (AVP)- and VIP-positive neurons (Fig. 2*C*), which are markers, respectively, of shell and core SCN subdivisions. A distinctive feature of the circadian behavior of *mPer*-based reporters is their spatiotemporal "wave" by which bioluminescent or fluorescent activity progresses across the SCN from the dorsomedial shell to the ventrolateral core (11, 12, 20). It is not known whether this dynamic is a unique feature of *mPer* expression, possibly reflecting CRE-mediated activation of *Per* by interneuronal cues, or a conserved aspect of the complete molecular cycle. If the latter, the wave would be common to all components of the pacemaker, including *mCry1*. Analysis of regional *mCry1-luc* bioluminescence highlighted a wave emanating from a leading edge in the dorsomedial lip of the SCN (Fig. 2*D*, Fig. S2, and Movie S1). The activity in this region was advanced by

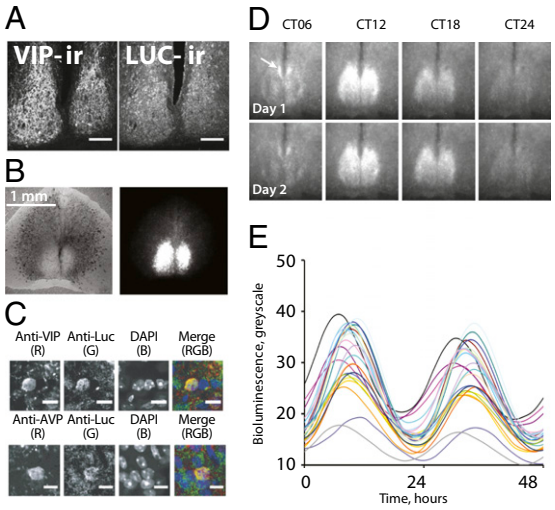

Fig. 2. Spatiotemporal control of *mCry1* circadian activation across the SCN circuit. (*A*) Confocal photomicrographs (magnification of 20×) reveal *mCry1*-driven luciferase immunoreactivity (-ir) across the SCN, delineated by VIP expression. (Scale bar: 100 μm.) (*B*) Organotypic SCN slice viewed in phase (*Left*) or as *mCry1-luc* bioluminescence (*Right*). (*C*) High-power (magnification of 63×) confocal images reveal expression of *mCry1*-driven luciferase in both VIP- (*Upper*) and AVP-immunoreactive (*Lower*) SCN neurons. (Scale bar: 10 μm.) (*D*) Serial frames from a representative slice demonstrate circadian expression of *mCry1* across SCN over 2 d. Arrow indicates phase-leading dorsomedial lip. (*E*) Representative plots of circadian bioluminescence recorded from individual SCN cells by CCD.

approximately 2.30 ± 0.13 h relative to the remainder of the SCN [assessed by fast Fourier transform (FFT)]. Similarly, bioluminescence rhythms of individual cells were clearly synchronous but with a distribution of phases (Fig. 2*E* and Fig. S2), and, when assigned into phase groups, cells in the dorsomedial lip were advanced by between 1.16 ± 0.28 h and 3.77 ± 0.15 h relative to laterally and ventrally placed cells, respectively. The *mCry1-luc* reporter therefore demonstrates that the spatiotemporal wave across the SCN circuitry is not exclusively a CRE-dependent phenomenon. Rather, it is a feature of both components of the negative feedback axis, *mPer* and *mCry*; and may arise from temporally and spatially sequential activation of E-box–mediated transcription.

Circadian Regulation of mCry1 by VIP/VPAC2 Signaling. The neuropeptide VIP and its receptor, VPAC2, are necessary to maintain the amplitude and synchrony of *mPer*-reported molecular pacemaking (21, 22). The VPAC2 receptor stimulates cAMP synthesis, thereby maintaining the amplitude and synchrony of *Per* expression via CREs in the *mPer* genes. The degree to which the loss of VIP/VPAC2 signaling compromises other components of the molecular pacemaker is unknown. If E-box–directed circadian expression of *mCry1* is independent of cAMP/mPER proteins, loss of VIP/VPAC2 signaling would not affect *mCry1-luc* rhythms. To test this directly, *mCry1-luc* mice were crossed onto VIP- or VPAC2-null backgrounds (Fig. 3*A*). Mean bioluminescence levels were comparable between WT and VPAC2-null heterozygous slices (2,940 ± 403 cps, $n = 28$; 2,759 ± 463 cps, $n = 11$). Bioluminescence tended to be lower in VPAC2-null homozygous slices (2,010 ± 399, $n = 9$; $P > 0.05$) and was significantly lower in VIP-null slices (622 ± 120, $n = 7$; $P < 0.01$). FFT analysis was nevertheless able to define periodicity in the recordings from VPAC2-null SCN (24.27 ± 0.40 h) that was not significantly different from WT (24.21 ± 0.09 h) or VPAC2-null heterozygotes (23.92 ± 0.13 h). The period of VIP-null SCN was, however, statistically longer than WT (25.18 ± 0.61; $P < 0.05$). More significantly, there was a rapid damping of the circadian pattern in VIP- and VPAC2-null SCN, such that the oscillation progressively lost definition, and errors of period and relative amplitude were greater (Fig. 3*B*).

To determine the cause of these disorganized rhythms, *mCry1-luc* emission was imaged with CCD cameras. In WT SCN, cellular rhythms were highly synchronous, as revealed by the Rayleigh analysis (Fig. 3 *C* and *D*): the small spread in phases reflecting the spatiotemporal wave. In contrast, cellular rhythms in VPAC2- and VIP-null slices were poorly synchronized, with Rayleigh plots having low or null statistical significance and reduced mean vectors. This loss of synchrony mirrors that shown with *mPer*-based reporters. To test this further, VPAC2-null, *mCry1-luc* SCN slices were treated with forskolin (20 μM), which is known to transiently restore circadian organization to *Per* expression in VPAC2-null SCN (21). Forskolin triggered a transient increase in bioluminescence levels, associated at the cellular level

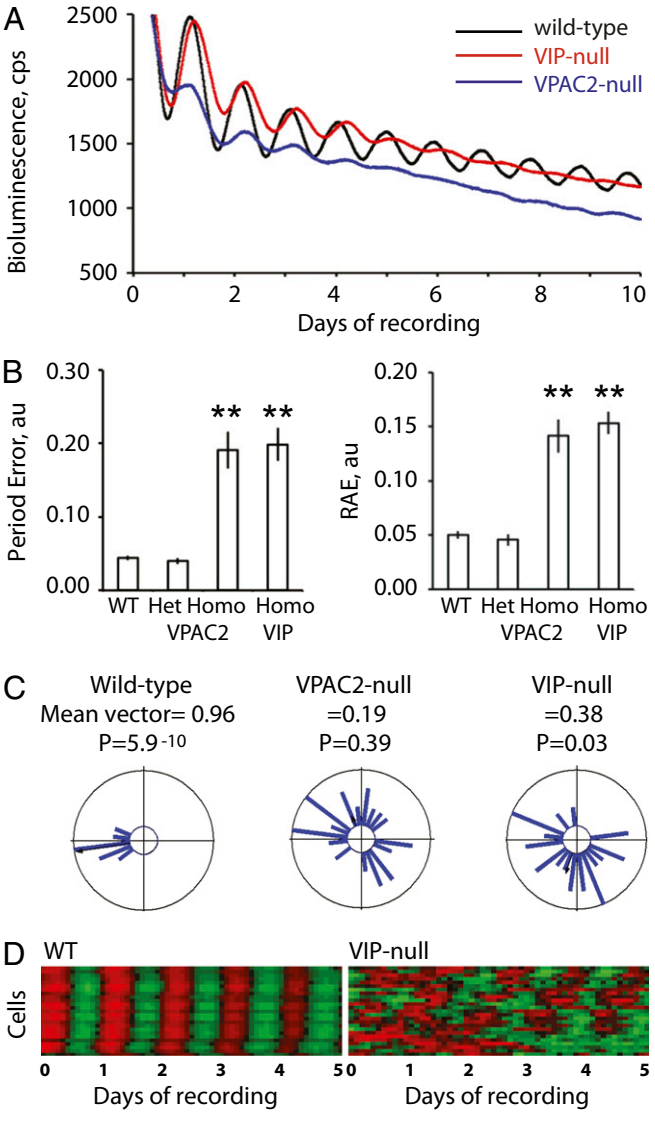

Fig. 3. Circadian regulation of *mCry1* by interneuronal VIP/VPAC2 signaling. (*A*) Representative bioluminescence recordings from WT, VPAC2-null, or VIP-null *mCry1-luc* SCN. (*B*) Group data (mean ± SEM) for period error (*Left*) and RAE (*Right*) of *mCry1-luc* bioluminescence rhythms from WT and VPAC2- or VIP-null SCN. (**$P < 0.01$ vs. WT by ANOVA and post-hoc Bonferroni correction.) (*C*) Rayleigh plots ($n = 25$) of cellular bioluminescence rhythms from representative WT and VPAC2- and VIP-null SCN. (*D*) Raster plots of cellular *mCry1-luc* bioluminescence rhythms from representative WT and VIP-null SCN recorded by CCD over 5 d.

NEUROSCIENCE

with resynchronized rhythmic expression (Fig. S3*A*). Thus, *mCry1* expression was perturbed by upstream deficiencies in VIP/VPAC2 and compromised cAMP signals.

Indirect Regulation of SCN mCry1 by cAMP Signaling. To test directly the dependence of *mCry1* expression on cAMP, SCNs were treated with MDL-12,330A (1 μM), which inhibits AC and reversibly suppresses cAMP levels in the SCN, thereby curtailing CRE activation and *mPer1*/*mPer2* expression (19). Vehicle-treated slices ($n = 5$) displayed the typical progressive decline in bioluminescence levels, falling by 73.8 ± 3.8% during the 5 d (Fig. 4*A*). The amplitude of the oscillation also decreased to 69 ± 11%. With addition of MDL, however, there was a dramatic and significant decrease in bioluminescence to 45.6 ± 1.7% of pretreatment level (n = 7; $P < 0.01$, *t* test) and amplitude to 22 ± 3% (*t* test, $P < 0.01$). The period of oscillation was not affected (vehicle, 23.75 ± 0.26 h; vs. MDL, 24.32 ± 0.26 h), but the coherence was reduced by MDL (RAE before, 0.038 ± 0.006; after, 0.096 ± 0.014; $P < 0.01$, *t* test) and not by vehicle (RAE before, 0.026 ± 0.002; after, 0.028 ± 0.002). After MDL washout, the SCN reestablished circadian rhythms comparable to those seen before treatment. Thus, inhibition of AC reversibly suppressed the absolute level of *mCry1* activation, damped the amplitude, and reduced coherence of the oscillation. Circadian *mCry1-luc* expression therefore requires competent cAMP/CRE signaling.

To explore further the role of cAMP/CRE signaling in *mCry1* expression, SCNs from mPER2::LUC or *mCry1-luc* mice were treated with forskolin (20 μM) to activate AC. In mPER2::LUC slices, forskolin acutely induced PER2 protein (relative change in bioluminescence over 24 h following treatment, mPER2::LUC vehicle, 0.92 ± 0.02; forskolin, 1.37 ± 0.08; $n = 6$; $P < 0.0.01$, *t* test; Fig. 4*B*). No such acute effect was apparent in *mCry1-luc* slices (vehicle, 0.90 ± 0.02; forskolin, 0.86 ± 0.02; $n = 7$). Rather, *mCry1-luc* activity was suppressed on the first nadir after addition of forskolin ($P < 0.01$, vehicle vs. forskolin, paired *t* test; $n = 7$; Fig. 4*C*). This occurred subsequent to the surge in mPER2 protein levels in the parallel mPER2::LUC slices. The elevated mPER2::LUC expression progressively damped with prolonged treatment (Fig. 4 *B* and *D*). Comparable damping was seen in the *mCry1-luc* oscillation, such that, after six cycles, the peak amplitude for both reporters was significantly suppressed relative to vehicle-treated slices (ANOVA, $P < 0.01$; $n = 3$ per group; Fig. 4*D*). Circadian regulation of *mCry1* expression is therefore indirectly dependent on cAMP-dependent signaling. Although *mCry1-luc* did not share the acute CRE-mediated sensitivity of mPER2::LUC to altered cAMP levels, the acute increase and long-term damping of mPER expression arising from elevated cAMP levels fed forward to dysregulate E-box–dependent *mCry1-luc* rhythms.

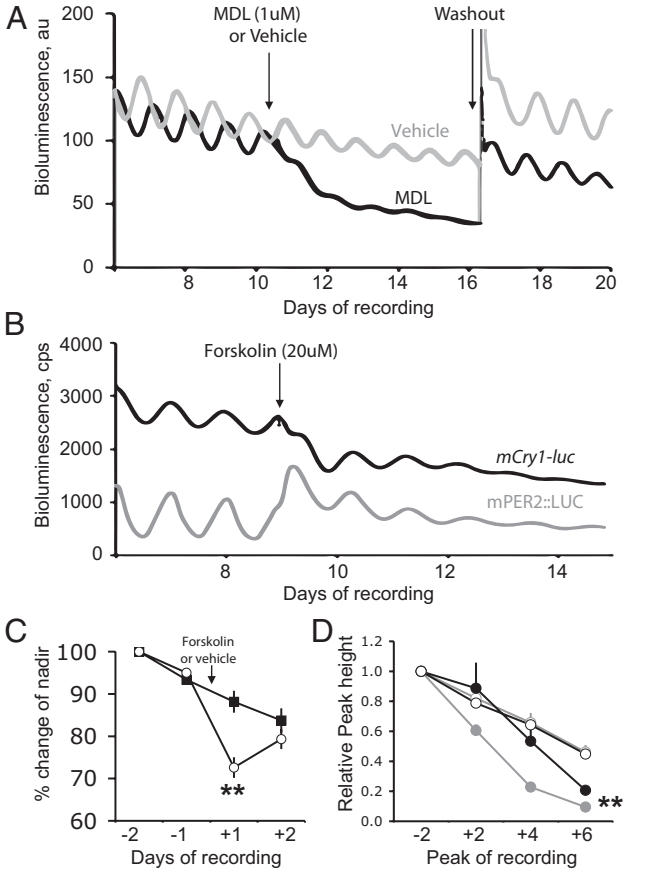

Fig. 4. Indirect regulation of *mCry1* expression in the SCN by cAMP-mediated signaling. (*A*) Representative bioluminescence plots from *mCry1-luc* SCN treated with vehicle or AC inhibitor MDL-12,330A for 5 d and then subjected to medium change. Plots normalized to 100% at time of treatment. (*B*) Representative bioluminescence plots from *mCry1-luc* and mPER2::LUC SCN treated with forskolin. (*C*) Effect of forskolin (closed) or vehicle (open) on nadir of bioluminescence of *mCry1-luc* SCN (mean ± SEM, $n = 7$ for both treatments). (*D*) Effect of forskolin (closed circles) or vehicle (open circles) on relative peak height of bioluminescence of mPER2::LUC (gray) or *mCry1-luc* (black) SCN (mean ± SEM, $n = 3$ for all conditions). (**$P < 0.01$ vs. vehicle-treated SCN, ANOVA and post-hoc Bonferroni correction.)

Circadian Control of mCry1-luc Expression by mPER1/mPER2. To test the presumed role of PER proteins in the indirect control of *mCry1* by intercellular cues, the *Cry1-luc* reporter mouse was crossed to an mPER1/mPER2-null background. These mice are behaviorally arrhythmic (23) and, at the level of the SCN, molecular pacemaking was severely compromised (Fig. 5*A*). In some slices ($n = 4$), no significant rhythm of *mCry1-luc* expression was detectable by FFT. In others ($n = 6$), a weak, short period oscillation (20.36 ± 1.81 h) persisted for four or five cycles. The oscillation had low amplitude [35.39 ± 17.63 vs. 403 ± 49 (WT)] and was poorly organized (RAE, 0.361 ± 0.175; vs. WT, 0.050 ± 0.004). Thus, E-box–mediated circadian *mCry1* expression in the SCN is dependent on mPER1/2.

To test the presumed role of PER proteins as transducers of cAMP signals onto *mCry1* expression, mPER1/2-null SCNs were treated with forskolin (20 μM). In contrast to the suppression of *mCry1*-driven bioluminescence observed in WT slices, forskolin caused a small (*ca.* 10%) increase in emission in mPER1/2-null SCN over the subsequent 24 h (Fig. S3*B*). In the absence of PER proteins, this brief activation of *mCry1-luc* was not accompanied by the transient restoration of circadian oscillation noted earlier with the PER-proficient VIP-null SCN. The weak response was not a consequence of the mPER1/2-null background per se, because, in mPER1/2-null SCN carrying a *mPer1-luc* reporter, forskolin triggered a >50% increase in bioluminescence that persisted for several days (Fig. S3*B*). Thus, cAMP-dependent signals can be activated in mPER1/2-null SCN, so the absence of cAMP-dependent suppression of *mCry1* was likely caused by the absence of cAMP-inducible PER proteins to act upon E/E′-boxes of the *mCry1* reporter.

Having demonstrated the contribution of PER proteins to circadian/cAMP control of *mCry1* expression, we tested whether mPER1/2 are the only transducers for *mCry1*. To address this, we applied our SCN graft procedure (4), which previously highlighted VPAC2-dependent and -independent mechanisms for synchronization of circadian mPER2 expression. To confirm that SCN grafts can restore circadian *mCry1-luc* expression, VIP-null slices were recorded by PMT for approximately 10 d, by which time *mCry1* rhythms had damped. A WT SCN was then grafted onto the mutant host. As seen previously with the mPER2::LUC reporter, the graft restored more coherent and higher high-amplitude *mCry1*-driven bioluminescence in the host SCN (Fig. S3*C*), confirming the earlier conclusion that extracellular cues are able, indirectly, to control *mCry1* circadian expression. We

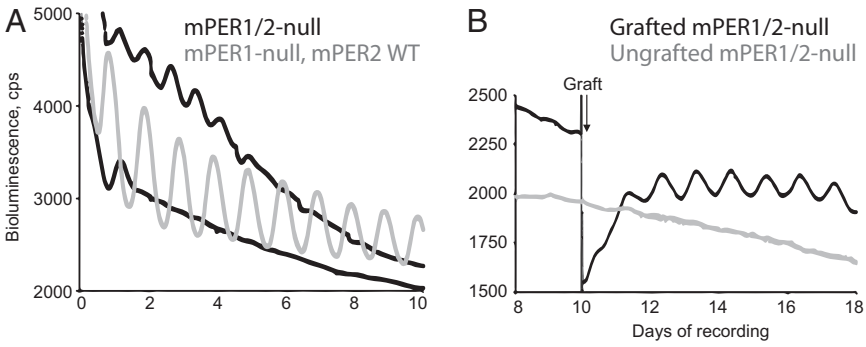

Fig. 5. Circadian control over *mCry1* expression by mPER1 and mPER2. (*A*) Representative bioluminescence plots from mPER1/2-null *mCry1-luc* SCN, one immediately arrhythmic and the other with transient short period cycles. A reference plot from a representative mPER1-null mPER2 WT slice is included. (*B*) Representative bioluminescence plots from mPER1/2-null *mCry1-luc* SCN that did or did not receive a WT SCN graft.

then tested the effect of grafting onto mPER1/2-null SCN. As noted earlier, these slices were arrhythmic before grafting. In slices that did not receive a graft ($n = 3$), residual rhythms were of very low amplitude (3.39 ± 0.62) and poorly organized (RAE, 0.288 ± 0.037; Fig. 5*B*). Forty-eight hours after grafting of a WT SCN onto the host, clear circadian rhythmicity was restored (period, 23.64 ± 0.31 h; $n = 6$). Graft-driven rhythmicity was of higher amplitude (39.06 ± 5.29) and better organized (RAE, 0.109 ± 0.043) than in nongrafted slices, and continued for the duration of recording (>10 d; all $P < 0.01$). Thus, in the absence of mPER1 and mPER2, circadian expression of *mCry1* can be restored by extracellular cues. Importantly, the resulting oscillations were of lower amplitude than the spontaneous rhythms of WT SCN noted earlier (403 ± 49), and were less well defined (WT RAE, 0.050 ± 0.004). Nevertheless, our results reveal the contribution of PER-independent as well as PER-dependent mechanisms to circadian expression of *mCry1*.

Discussion

mCRY1 is the principal negative regulator within the feedback loops that define circadian time (2, 17), so description of the dynamics of its expression in the SCN is central to understanding the timekeeping mechanism. This study therefore developed a bioluminescent reporter mouse with which to monitor E-box–dependent circadian regulation of *mCry1* to extend our view of the molecular clockwork beyond the existing *Per*-based constructs. We then used the mouse to investigate the mechanisms that direct circadian expression of *mCry1*, in particular to determine how *mCry1* expression is synchronized within and between SCN neurons. The B6.Cg-Tg(Cry1-luc)^{01Ld} line provided a high-fidelity, real-time report of SCN *mCry1* expression, with appropriate phase, period, and profile. CCD imaging showed that a coordinated spatiotemporal wave of expression is a feature of both components of the negative feedback axis: *Cry* as well as *Per*. Despite lacking CRE sequences, *mCry1* expression was dependent on VIP/VPAC2 interneuronal cues and intraneuronal cAMP signaling, highlighting indirect circadian regulation. Moreover, mPER1 and mPER2 proteins were necessary transducers for circadian and cAMP-mediated regulation of *mCry1*. By using an SCN graft procedure, we showed that PER-independent as well as PER-dependent mechanisms sustain circadian expression of *mCry1*. The B6.Cg-Tg(Cry1-luc)^{01Ld} mouse therefore provides a unique view upon *mCry1* expression and its interaction with PER at the heart of the circadian pacemaker.

Although overall bioluminescence levels were not different between *mCry1-luc* and mPER2::LUC SCN, the amplitude of oscillation was smaller in *mCry1-luc* tissue, as noted in vivo (17). Furthermore, consistent with the previous validation of the *mCry1* sequence for circadian reporting in fibroblasts (13), the B6.Cg-Tg(Cry1-luc)^{01Ld} reporter was useful for the analysis of circadian expression in peripheral tissues and MEFs, albeit less well defined than the mPER2::LUC reporter. Importantly, the principal circadian elements of the mCry1-luc reporter are the E-box and E′-box (13), which provide a readout for activation within the central circadian feedback loop. In addition, the E′-box incorporates two overlapping D-box motifs (14), which may moderately tune its activity in terms of phase and amplitude. The reporter does not, however, contain the intronic RORE sequences, which have been shown in cell-based assays to be capable of conferring a marked phase delay of approximately 4 h to the oscillation (14). The E-boxes, on the contrary, were sufficient to recapitulate in the SCN slice a phase of circadian *mCry1* expression, relative to *mPer1*, that replicated their in vivo expression. Thus, whereas the intronic ROREs are reported as necessary to determine *mCry1* phase in cells (14) and peripheral tissues (24; but see ref. 13), they were clearly not required for appropriate phase control in the SCN. The effects of Fbxl3^{Afh}, in which CRY protein degradation is impaired, further emphasized the fidelity of the reporter as a readout of E-box–mediated gene expression. *mCry1-luc* reported the molecular signature of the Afh mutant mice: prolonged negative feedback onto the E/E′-boxes arising from stabilized mCRY.

The reporter provided explicit insights into the role of interneuronal communication in driving the core clockwork. Previous analyses have relied on *Per*-based reporters, but these carry both E-boxes and CREs, so activity arising from acute interneuronal signals (via CREs) would confound analysis of sustained circadian cycles (via E-boxes). CCD recording revealed that *mCry1* activation followed a spatiotemporal wave that was initiated at the dorsomedial lip of the SCN and processed ventrally and laterally (11). Although this wave is initiated by localized cAMP-dependent signals (25), consistent with actions on *Per* expression, the present study shows that the wave is shared by other components of the feedback loop. Future studies with the *mCry1-luc* mouse will seek to identify the dependence of the wave on PER-dependent signals. Thus, different spatially specified neuronal populations of the SCN encode temporally specific oscillations, adding a further layer of circuit-level complexity to the control of E-box–dependent SCN outputs. The role of interneuronal cues in specifying this phase structure was evident in the progressive damping of circadian *mCry1* expression and loss of cellular synchrony in VIP- and VPAC2-null SCN. Previous in situ hybridization assays of steady-state *mCry1* expression in the VPAC2-null SCN showed little change in mean expression level but a loss of rhythmicity (26). The reporter now shows that loss of cellular synchrony of *mCry1* expression is the cause of this phenotype. It also shows that VPAC2-dependent signaling has access into the core clockwork beyond the CREs of *Per*, as highlighted by the restoration of *mCry1* rhythms in mPER1/2-null SCN by grafts of WT SCN. Importantly, this restoration demonstrates that the paracrine mechanisms that drive circadian-incompetent SCN (4) really can address the entire oscillatory system, rather than simply stimulating the *Per*-based reporters via their CREs but having no downstream consequences.

Sensitivity to manipulations of AC/cAMP revealed an indirect pathway whereby VIP/VPAC2 and other interneuronal signals can direct *mCry1* rhythms. The serial responses of mPER2::LUC and *mCry1* to forskolin provided correlative evidence that PER proteins act as transducers in such a pathway, their elevation subsequently suppressing E-box activation of *mCry1*. Evidence of

a necessary role was seen in mPER1/2-null SCN: *mCry1* expression damped rapidly and activation of cAMP signaling no longer suppressed *mCry1*. It should be noted, however, that the mPER1 and mPER2 proteins are not the sole means of extracellular control over circadian *mCry1* expression because a WT graft restored circadian expression of *mCry1* in mPER1/2-null SCN. Although we did not specifically address any contribution from PER3, this is an unlikely mediator of this effect because it is neither necessary nor sufficient for circadian function; it does not carry CREs and is not acutely regulated by extracellular cues (23). If PER-independent regulation of *mCry1* is mediated by other components of the feedback loop, DBP, acting via the D-boxes (14), is a candidate, although, as with *mPer3*, it does not carry CREs. In contrast, DEC-1, a factor that suppresses CLOCK/BMAL1 activity at E-boxes, does carry CREs (27). Alternatively, metabolic, redox-dependent cues may play a role. It is now well established that the transcriptional loops are intermeshed with cycles of cellular metabolism (28), and the SCN slice in culture expresses a marked circadian cycle of superoxidation of peroxiredoxin proteins (29). Whether such metabolic cues are capable of driving the core loop in the absence of PER proteins remains to be determined, but there is growing evidence that cytosolic processes can cycle independently of, and influence the behavior of, the transcriptional feedback loops (30). Transient circadian cycles were evident in mPER1/2-null SCN in the present study, and have also been reported in BMAL1- (31) and CRY1/2-null SCN (4), indicative of ongoing cytosolic oscillations. Circadian control of *mCry1* by the SCN graft in the mPER1/2-null SCN may involve such "cytoscillators" (30). In conclusion, therefore, the creation and subsequent analysis of the B6.Cg-Tg(Cry1-luc)^{01Ld} mouse has provided a unique perspective on inter- and intracellular pathways (Fig. S4) that act on the fulcrum of the core circadian pacemaker: E-box–mediated expression of the principal negative regulator, mCRY1 (2).

Materials and Methods

All animal work was licensed under the UK Animals (Scientific Procedures) Act of 1986 with local ethical approval. To create transgenic mice we used a *mCry1* sequence (−1,504 to +107; Fig. S1*A*) equivalent to ovine sequence previously shown to sustain circadian bioluminescence when transfected as a plasmid into fibroblasts (13). The transgenic fragment was excised by using EcoR1 and Sal1 and injected into the pronuclei of fertilized eggs (B6CBAF1/OlaHsd strain). Six potential founder mice were identified by PCR analysis, whereby a 250-bp band from the luciferase transgene was amplified with primers 5′ CTT CAG AAA CGT GAG GTG CCG 3′ and 5′ AGC GTA AGT GAT GTC CAC CTC G 3′. One line was selected for further use and crossed with WT and circadian mutant lines from our in-house colonies all with a C57Bl6 background C57Bl6 (more than six back-crosses to C57Bl6). Copy number was determined by QX100 Droplet Digital PCR (Bio-Rad). SCN organotypic slices were routinely made from 5- to 12-d-old pups, and bioluminescence recorded after at least 7 d in culture by using photomultiplier arrays or CCD camera as described previously (21). Luciferin-EF (Promega) was added at an initial concentration of 0.1 μM. Peripheral tissue explants were recorded immediately under PMTs, and primary fibroblasts were prepared from *mCry1-luc* and mPER2::LUC embryos (embryonic day 13–14) and maintained in DMEM supplemented with 10% (vol/vol) FBS before plating in 35-mm dishes at $\sim 1 \times 10^6$ cells per dish in Hepes-buffered medium (20). Data were analyzed by using IPLab and Oriana software (4) and the FFT–nonlinear least squares algorithm, accessed through the BioDare database (www.biodare.ed.ac.uk). The first 24 h of data were discarded to avoid experimental artifacts. For single-cell analysis, CCD images were converted to 8-bit image stacks by using ImageJ (National Institutes of Health) and analyzed by using Semiautomated Routines for Functional Image Analysis plug-in component within Igor-Pro (Wavemetrics) data analysis software. Single cells were identified by the automated region of interest (ROI) selection tool. Bioluminescence intensity in grayscale values was extracted from all ROIs above 0.4 threshold and 6 μm diameter, to select for "cell-like" ROIs. Bioluminescence intensity units were generated for each ROI through the image stack and visualized in a raster plot. Immunofluorescent staining with goat anti-luciferase (1:1,000; Promega), rabbit anti–[Arg8]-vasopressin, and guinea pig anti-VIP (1:1,000; Bachem) and graft cocultures were conducted as described previously (4, 20). Drugs (forskolin, IBMX, and MDL-12,330A) were obtained from Sigma-Aldrich.

ACKNOWLEDGMENTS. We thank Dr. Tomasz Zielinski for expert assistance with BioDare, Mr. P. Margiotta for assistance with figures, and LMB Biomedical Services Group for animal care. This work was supported by Medical Research Council (United Kingdom). BioDare is supported by Biotechnology and Biological Sciences Research Council and Engineering and Physical Sciences Research Council Awards BB/D019621, BB/F59011/1, and BB/F005237/1 to SynthSys and ROBuST (University of Edinburgh).

1. Hastings MH, Reddy AB, Maywood ES (2003) A clockwork web: Circadian timing in brain and periphery, in health and disease. *Nat Rev Neurosci* 4(8):649–661.
2. Koike N, et al. (2012) Transcriptional architecture and chromatin landscape of the core circadian clock in mammals. *Science* 338(6105):349–354.
3. Ueda HR, et al. (2005) System-level identification of transcriptional circuits underlying mammalian circadian clocks. *Nat Genet* 37(2):187–192.
4. Maywood ES, Chesham JE, O'Brien JA, Hastings MH (2011) A diversity of paracrine signals sustains molecular circadian cycling in suprachiasmatic nucleus circuits. *Proc Natl Acad Sci USA* 108(34):14306–14311.
5. An S, Irwin RP, Allen CN, Tsai C, Herzog ED (2011) Vasoactive intestinal polypeptide requires parallel changes in adenylate cyclase and phospholipase C to entrain circadian rhythms to a predictable phase. *J Neurophysiol* 105(5):2289–2296.
6. Güler AD, et al. (2008) Melanopsin cells are the principal conduits for rod-cone input to non-image-forming vision. *Nature* 453(7191):102–105.
7. Hastings MH, et al. (1996) Entrainment of the circadian clock. *Prog Brain Res* 111: 147–174.
8. Travnickova-Bendova Z, Cermakian N, Reppert SM, Sassone-Corsi P (2002) Bimodal regulation of mPeriod promoters by CREB-dependent signaling and CLOCK/BMAL1 activity. *Proc Natl Acad Sci USA* 99(11):7728–7733.
9. Shigeyoshi Y, et al. (1997) Light-induced resetting of a mammalian circadian clock is associated with rapid induction of the mPer1 transcript. *Cell* 91(7):1043–1053.
10. Reddy AB, Field MD, Maywood ES, Hastings MH (2002) Differential resynchronisation of circadian clock gene expression within the suprachiasmatic nuclei of mice subjected to experimental jet lag. *J Neurosci* 22(17):7326–7330.
11. Yamaguchi S, et al. (2003) Synchronization of cellular clocks in the suprachiasmatic nucleus. *Science* 302(5649):1408–1412.
12. Yoo SH, et al. (2004) PERIOD2:LUCIFERASE real-time reporting of circadian dynamics reveals persistent circadian oscillations in mouse peripheral tissues. *Proc Natl Acad Sci USA* 101(15):5339–5346.
13. Fustin JM, O'Neill JS, Hastings MH, Hazlerigg DG, Dardente H (2009) Cry1 circadian phase in vitro: wrapped up with an E-box. *J Biol Rhythms* 24(1):16–24.
14. Ukai-Tadenuma M, et al. (2011) Delay in feedback repression by cryptochrome 1 is required for circadian clock function. *Cell* 144(2):268–281.
15. Meng QJ, et al. (2008) Setting clock speed in mammals: The CK1 epsilon tau mutation in mice accelerates circadian pacemakers by selectively destabilizing PERIOD proteins. *Neuron* 58(1):78–88.
16. Godinho SI, et al. (2007) The after-hours mutant reveals a role for Fbxl3 in determining mammalian circadian period. *Science* 316(5826):897–900.
17. Kume K, et al. (1999) mCRY1 and mCRY2 are essential components of the negative limb of the circadian clock feedback loop. *Cell* 98(2):193–205.
18. Field MD, et al. (2000) Analysis of clock proteins in mouse SCN demonstrates phylogenetic divergence of the circadian clockwork and resetting mechanisms. *Neuron* 25(2):437–447.
19. O'Neill JS, Maywood ES, Chesham JE, Takahashi JS, Hastings MH (2008) cAMP-dependent signaling as a core component of the mammalian circadian pacemaker. *Science* 320 (5878):949–953.
20. Hastings MH, Reddy AB, McMahon DG, Maywood ES (2005) Analysis of circadian mechanisms in the suprachiasmatic nucleus by transgenesis and biolistic transfection. *Methods Enzymol* 393:579–592.
21. Maywood ES, et al. (2006) Synchronization and maintenance of timekeeping in suprachiasmatic circadian clock cells by neuropeptidergic signaling. *Curr Biol* 16(6):599–605.
22. Atkinson SE, et al. (2011) Cyclic AMP signaling control of action potential firing rate and molecular circadian pacemaking in the suprachiasmatic nucleus. *J Biol Rhythms* 26(3):210–220.
23. Bae K, et al. (2001) Differential functions of mPer1, mPer2, and mPer3 in the SCN circadian clock. *Neuron* 30(2):525–536.
24. Etchegaray JP, Lee C, Wade PA, Reppert SM (2003) Rhythmic histone acetylation underlies transcription in the mammalian circadian clock. *Nature* 421(6919):177–182.
25. Doi M, et al. (2011) Circadian regulation of intracellular G-protein signalling mediates intercellular synchrony and rhythmicity in the suprachiasmatic nucleus. *Nat Commun* 2:327.
26. Harmar AJ, et al. (2002) The VPAC(2) receptor is essential for circadian function in the mouse suprachiasmatic nuclei. *Cell* 109(4):497–508.
27. Honma S, et al. (2002) Dec1 and Dec2 are regulators of the mammalian molecular clock. *Nature* 419(6909):841–844.
28. Bass J (2012) Circadian topology of metabolism. *Nature* 491(7424):348–356.
29. Edgar RS, et al. (2012) Peroxiredoxins are conserved markers of circadian rhythms. *Nature* 485(7399):459–464.
30. Hastings MH, Maywood ES, O'Neill JS (2008) Cellular circadian pacemaking and the role of cytosolic rhythms. *Curr Biol* 18(17):R805–R815.
31. Ko CH, et al. (2010) Emergence of noise-induced oscillations in the central circadian pacemaker. *PLoS Biol* 8(10):e1000513.